differences which although subtle are critical to an understanding of ionic conduction.

The above discussion is not intended to imply that constant-wavelength instruments are in general inferior to those based on time-of-flight. 'State-of-the-art' constant-wavelength instruments such as D2B would, we are sure, offer a considerably improved refinement to that from D1A, probably comparable in many respects to HRPD.

Finally, it is noteworthy that the X-ray structure determination (Plattner & Völlenkle, 1979) failed to identify the displaced Li(2a) cations or the existence of the second lithium site (4); this may be attributed to the weak scattering of X-rays by lithium ions.

We wish to thank R. M. Ibberson at the Neutron Division, Rutherford–Appleton Laboratory, England, for his help with data collection; the Computer Centre at Heriot-Watt University for provision of computer facilities for carrying out the refinements; and the SERC for financial support.

References

Abrahams, I., Bruce, P. G., David, W. I. F. & West, A. R. (1988). *J. Solid State Chem.* **75**(2), 390–396.

Bruce, P. G. & West, A. R. (1980). *Mater. Res. Bull.* **15**, 379–385.

Bruce, P. G. & West, A. R. (1982). *J. Solid State Chem.* **44**, 354–365.

Bruce, P. G. & West, A. R. (1984). *J. Solid State Chem.* **53**, 430–434.

David, W. I. F., Akporiaye, D. E., Ibberson, R. M. & Wilson, C. C. (1988). *The High Resolution Powder Diffractometer at ISIS – an Introductory Users Guide*, version 1.0. Rutherford–Appleton Laboratory, England.

Fitch, A. N., Fender, B. E. F. & Talbot, J. (1984). *J. Solid State Chem.* **55**, 14–22.

Hong, Y.-P. (1978). *Mater. Res. Bull.* **13**, 117–124.

International Tables for Crystallography (1983). Vol. A. Dordrecht: Kluwer Academic Publishers.

Koester, L. & Rauch, H. (1981). Report 2517/RB. International Atomic Energy Agency, Vienna.

Plattner, E. & Völlenkle, H. (1979). *Monatsh. Chem.* **110**, 693–698.

Rietveld, H. M. (1969). *J. Appl. Cryst.* **2**, 65–71.

Rodger, A. R., Kuwano, J. & West, A. R. (1985). *Solid State Ionics*, **15**, 185–198.

West, A. R. & Bruce, P. G. (1982). *Acta Cryst.* **B38**, 1891–1896.

Zeman, J. (1960). *Acta Cryst.* **13**, 863–867.

Acta Cryst. (1989). B**45**, 462–466

Structural Analysis of the Threefold-Modulated Monoclinic Phase of $[N(CH_3)_4]_2ZnCl_4$

By F. J. Zúñiga, G. Madariaga and J. M. Pérez-Mato

Departamento de Fisica de la Materia Condensada, Facultad de Ciencias, Universidad del Pais Vasco, Apdo 644 *Bilbao, Spain*

(*Received* 9 *September* 1988; *accepted* 8 *May* 1989)

Abstract

The crystal structure of the threefold monoclinic low-temperature phase of bis(tetramethylammonium) tetrachlorozincate(II), $[N(CH_3)_4]_2ZnCl_4$, has been studied at 250 and 200 K. The R values are 0·062 (6893 reflections, 3616 observed) and 0·064 (1907 reflections, 1558 observed) at 250 and 200 K respectively. The distortion with respect to the high-temperature phase is analyzed in terms of symmetry modes, and compared with the distortion in the incommensurate phase. The mode with Σ_3 symmetry responsible for the normal–incommensurate transition is still predominant in the distortion. Crystal data: $M_r = 355{\cdot}5$, $\lambda(\text{Mo } K\alpha) = 0{\cdot}7107$ Å, $P2_1/n$, $Z = 12$, $F(000) = 2208$. At 250 K: $a = 8{\cdot}953\,(3)$, $b = 15{\cdot}456\,(10)$, $c = 36{\cdot}595\,(8)$ Å, $\gamma = 90{\cdot}19\,(4)°$, $V = 5064\,(6)$ Å^3, $D_x = 1{\cdot}40$ g cm^{-3}, $\mu = 20{\cdot}7$ cm^{-1}. At 200 K: $a = 8{\cdot}960\,(2)$, $b = 15{\cdot}309\,(5)$, $c = 36{\cdot}628\,(8)$ Å, $\gamma = 90{\cdot}46\,(2)°$, $V = 5024(4)$ Å^3, $D_x = 1{\cdot}41$ g cm^{-3}, $\mu = 21{\cdot}0$ cm^{-1}.

1. Introduction

Bis(tetramethylammonium) tetrachlorozincate (TMATC-Zn) is one of the most studied compounds of the A_2BX_4 family having a one-dimensional incommensurate (INC) phase. This compound undergoes five solid–solid phase transitions:

$$\mathrm{I} \xrightarrow[T_i]{297\ \mathrm{K}} \mathrm{II} \xrightarrow[T_c]{281\ \mathrm{K}} \mathrm{III} \xrightarrow{277\ \mathrm{K}} \mathrm{IV} \xrightarrow{171\ \mathrm{K}} \mathrm{V} \xrightarrow{159\ \mathrm{K}} \mathrm{VI},$$

where the temperatures are those obtained from calorimetric measurements by Ruiz-Larrea, Lopez-Echarri & Tello (1981).

Diffraction patterns of phases II, III and IV show superstructure reflections along the **c*** direction that correspond to periodicities of $\sim 5c_0$ (INC), $5c_0$ and $3c_0$ respectively, c_0 being the lattice constant of phase I (Tanisaki & Mashiyama, 1980). These satellite reflections are all weak and the structures can be considered small distortions of the parent phase I.

The structure of phase I (basic structure, space group *Pmcn*) was determined by Wiesner, Srivastava, Kennard, Di Vaira & Lingafelter (1967). The structures of phase II [INC phase, superspace group $P(Pmcn)$:$(s1\bar{1})$] and the ferroelectric phase III (lock-in phase, space group $P2_1cn$) have been reported by Madariaga, Zúñiga, Pérez-Mato & Tello (1987).

Using phenomenological approaches, Mashiyama (1980) obtained the order-parameter symmetry characterizing the phase-transition sequence. The order parameter is associated with a modulation having the transformation properties of the irreducible representation Σ_3 with a wavevector $\mathbf{k} = \alpha\mathbf{c}^*$, where α takes different values in each phase. In phase III the modulation wavevector locks at the value of $2/5\mathbf{c}^*$, whereas in phase IV α takes the value 1/3.

The structural analysis of the INC and lock-in structures (phases II and III), reported in Madariaga, Zúñiga, Pérez-Mato & Tello (1987), demonstrated that the main part of the distortion describing phases II and III has Σ_3 symmetry and is practically the same in both structures except for the change of wavevector of the modulation and a small increase of the global amplitude.

Phase IV is a threefold structure with space group $P112_1/n$ (Tanisaki & Mashiyama, 1980). In this paper, two structure determinations of this phase at 250 and 200 K respectively are presented. The double determination is motivated by the high disorder found at 250 K which decreases at 200 K. The structural distortion describing this phase with respect to phase I is decomposed in its contributing modes. The most relevant components are compared with those of the INC phase. Despite the change of symmetry, the predominance of a Σ_3 modulation which in broad terms still keeps the same internal structure as in the INC phase is also observed in this phase.

2. Experimental

Single crystals of TMATC-Zn were grown by slow evaporation at room temperature from an aqueous solution containing $N(CH_3)_4Cl$ and $ZnCl_2$ in stoichiometric proportions. The structure has been analyzed at 250 and 200 K, with diffraction intensities collected from two different crystals. The measurements at 250 K were performed with a CAD-4 diffractometer equipped with an N_2-gas-flow cooling system (Cosier & Glazer, 1986), whereas for those at 200 K, a Syntex $P2_1$ diffractometer with an Enraf–Nonius low-temperature system was used. In both cases, when cooling through the III–IV transition, untwinned crystals were obtained. The stability of the measurements was checked periodically by measuring three standard reflections, and they were used to correct a mean intensity decay of 10 and 8% (at 250 and 200 K respectively) at the end of the measurements, which is attributeed to radiation damage. Table 1 summarizes the relevant crystal data and data-collection information for both measurements.

Table 1. *Summary of experimental data*

	250 K	200 K
Crystal shape	Prismatic	Sphere
Crystal size (mm)	0·1 × 0·2 × 0·15	0·22
Temperature stability (K)	0·2	1
Monochromator/filter	Graphite	Nb
Reflections for lattice constants	25 ($10 < \theta < 16$)	15 ($10 < \theta < 18$)
Scan	θ–2θ	θ 2θ
Scan speed (min^{-1})	4·12–0·5	10·0–2·0
Limits *h,k,l*	± 12,21,39	± 6,11,26
$(\sin\theta/\lambda)_{max}$ (Å^{-1})	0·70	0·367
Absortion correction (A^*)	None	1·35 1·34
Independent reflections	6893	1907
Observed reflections ($I > 3\sigma$)	3616	1558
Weights	$1/\sigma^2$	$1/\sigma^2$
Maximum (shift/e.s.d.)	0·86	0·23

3. Structure of phase IV

For the reduction of the X-ray measurments and the refinement of the structures, the *XRAY* system of programs (Stewart, Kruger, Ammon, Dickinson & Hall, 1972) was used. The intensities were corrected for Lorentz–polarization and absorption factors. In the structure-factor calculations, scattering factors for Zn^{2+}, Cl^-, N and C atoms were taken from Cromer & Mann (1968) and the anomalous-scattering corrections for Zn and Cl atoms were those of Cromer & Liberman (1970). H atoms were not considered in the refinements.

The structure at 250 K was refined by a block-diagonal least-squares method with anisotropic thermal parameters for all atoms. We used as starting parameters for the Zn and Cl atoms those of phase I extended over three consecutive cells. During the initial stages of the refinement a soft restriction for the Zn—Cl distances (prescribed to a value of 2·23 Å) was used. Successive Fourier maps revealed all the N and C atoms. The final residuals based on *F* were $R = 0{\cdot}062$ and $wR = 0{\cdot}063$ with $w = 1/\sigma^2(F)$. The goodness of fit was 2·28.* A final difference Fourier synthesis showed some peaks of 0·90 e Å^{-3} near the C(123) and C(124) atoms, but attempts to refine the structure with a splitting for these atoms failed. The atomic parameters of phase IV of TMATC-Zn at 250 K are reported in Table 2.

The structure at 200 K was refined including anisotropic thermal parameters for the Zn and Cl

---

* Lists of structure factors and anisotropic thermal parameters at 200 and 250 K, and bond lengths, bond angles and atomic parameters at 200 K have been deposited with the British Library Document Supply Centre as Supplementary Publication No. SUP 51876 (37 pp.). Copies may be obtained through The Executive Secretary, International Union of Crystallography, 5 Abbey Square, Chester CH1 2HU, England.

Table 2. *Atomic parameters of phase* IV *at* 250 K

The first appended numeral denotes the subcell of phase I. E.s.d.'s are given in parentheses. U_{eq} = 1/3(trace of the orthogonalized U_{ij} matrix).

	x	y	y	U_{eq} (Å^2)
Zn(1)	0·2552 (1)	0·40705 (8)	0·08153 (3)	0·0402 (5)
Cl(11)	0·2779 (3)	0·4047 (2)	0·02070 (9)	0·064 (1)
Cl(12)	0·2878 (3)	0·5423 (2)	0·1038 (1)	0·077 (1)
Cl(13)	0·4350 (3)	0·3228 (2)	0·1063 (1)	0·071 (1)
Cl(14)	0·0276 (3)	0·3551 (2)	0·09774 (9)	0·069 (1)
N(11)	0·2765 (7)	0·0935 (5)	0·0500 (2)	0·040 (3)
C(111)	0·249 (1)	0·0932 (9)	0·0911 (3)	0·090 (7)
C(112)	0·240 (1)	0·0083 (8)	0·0340 (3)	0·072 (5)
C(113)	0·180 (1)	0·1626 (9)	0·0312 (4)	0·099 (7)
C(114)	0·443 (1)	0·1131 (9)	0·0438 (4)	0·098 (7)
N(12)	0·2669 (8)	0·8263 (5)	0·1665 (2)	0·053 (4)
C(121)	0·251 (1)	0·7320 (9)	0·1540 (4)	0·123 (8)
C(122)	0·121 (2)	0·8611 (9)	0·1727 (6)	0·17 (1)
C(123)	0·345 (2)	0·876 (1)	0·1397 (6)	0·25 (2)
C(124)	0·346 (2)	0·830 (1)	0·1990 (6)	0·27 (2)
Zn(2)	0·2841 (1)	0·40727 (7)	0·41561 (3)	0·0387 (5)
Cl(21)	0·2658 (3)	0·4089 (2)	0·35430 (9)	0·076 (1)
Cl(22)	0·3239 (3)	0·5424 (2)	0·4378 (1)	0·075 (1)
Cl(23)	0·4781 (3)	0·3219 (2)	0·4323 (1)	0·068 (1)
Cl(24)	0·0692 (3)	0·3546 (2)	0·43914 (9)	0·071 (1)
N(21)	0·2532 (7)	0·0955 (5)	0·3835 (2)	0·056 (4)
C(211)	0·246 (2)	0·0989 (9)	0·4246 (4)	0·116 (9)
C(212)	0·204 (1)	0·0074 (7)	0·3705 (3)	0·087 (6)
C(213)	0·156 (2)	0·1648 (9)	0·3675 (4)	0·123 (8)
C(214)	0·416 (1)	0·110 (1)	0·3717 (4)	0·124 (8)
N(22)	0·2601 (7)	0·8277 (4)	0·4965 (2)	0·040 (3)
C(221)	0·405 (1)	0·8691 (7)	0·5092 (4)	0·079 (6)
C(222)	0·297 (1)	0·7382 (8)	0·4803 (4)	0·096 (6)
C(223)	0·155 (1)	0·8178 (8)	0·5279 (4)	0·110 (7)
C(224)	0·191 (1)	0·8810 (8)	0·4679 (4)	0·091 (6)
Zn(3)	0·2202 (1)	0·40342 (7)	0·74880 (4)	0·0385 (5)
Cl(31)	0·2062 (3)	0·4090 (2)	0·68757 (8)	0·065 (1)
Cl(32)	0·1866 (3)	0·5358 (2)	0·77431 (9)	0·068 (1)
Cl(33)	0·4483 (3)	0·3527 (2)	0·7657 (1)	0·070 (1)
Cl(34)	0·0387 (3)	0·3139 (2)	0·7696 (1)	0·071 (1)
N(31)	0·2270 (7)	0·0910 (5)	0·7155 (2)	0·044 (3)
C(311)	0·269 (1)	0·0034 (8)	0·7017 (4)	0·095 (7)
C(312)	0·257 (1)	0·0941 (8)	0·7554 (3)	0·092 (7)
C(313)	0·064 (1)	0·1093 (9)	0·7072 (3)	0·091 (6)
C(314)	0·322 (1)	0·1589 (8)	0·6968 (4)	0·091 (6)
N(32)	0·2216 (7)	0·8244 (5)	0·8312 (2)	0·046 (3)
C(321)	0·068 (1)	0·8478 (8)	0·8414 (4)	0·116 (8)
C(322)	0·320 (2)	0·8311 (9)	0·8641 (5)	0·151 (9)
C(323)	0·279 (2)	0·885 (1)	0·8028 (4)	0·133 (9)
C(324)	0·218 (1)	0·7338 (8)	0·8162 (4)	0·127 (9)

atoms but isotropic ones for N and C atoms. The final residual values obtained are $R = 0·064$ and $wR = 0·066$.*

The above-mentioned peaks in the difference Fourier synthesis at 250 K were at typical N—C distances of the N(12) atom. This fact, together with the large thermal parameters found for C(121), C(122), C(123) and C(124), points to a disorder for this tetramethylammonium group. The residual peaks persist at 200 K and even if the thermal parameters decrease, they continue to have anomalously large values of 0·16 and 0·15 Å^2 for C(123) and C(124). Relatively large values for the U_{11} thermal parameter are also found in the other organic groups indicating the existence of a disorder which in general is greater for the ions associated with N(12), N(22) and N(32). This result can be understood if we consider that in the structure the Cl atoms form two types of cages, one larger than the other, in which the tetramethylammonium ions are located. A similar result is found in the threefold structure of Rb$_2$ZnBr$_4$ where the Br cavity of the Rb(2) is considerably larger than that of Rb(1) (Hogervorst & Helmholdt, 1988).

4. Discussion

Projections of the structure (with C atoms excluded) in the *ac* plane at 250 K and at room temperature are shown in Fig. 1. Bond lengths and angles for phase IV at 250 K are given in Table 3. The most interesting feature of the structure is its distortion when referred to the 'basic' structure (phase I). If the small difference of the monoclinic angle from 90° is neglected, the structural distortion can be calculated by subtracting the coordinates of phase I given in Table 3 of Madariaga, Zúñiga, Pérez-Mato & Tello (1987) (in three consecutive cells) from those in Table 2. As a general result it can be concluded that for all atoms the x component of the atomic displacements is the most important. In the case of the atoms lying on the mirror plane in phase I it is even an order of magnitude higher than the y and z components.

A better insight into the structure can be obtained if the structural distortion is decomposed in terms of symmetry modes of the basic structure (phase I) as reported previously in other cases (Pérez-Mato, Gaztelua, Madariaga & Tello, 1986). This allows a more quantitative comparison with phases II(INC)

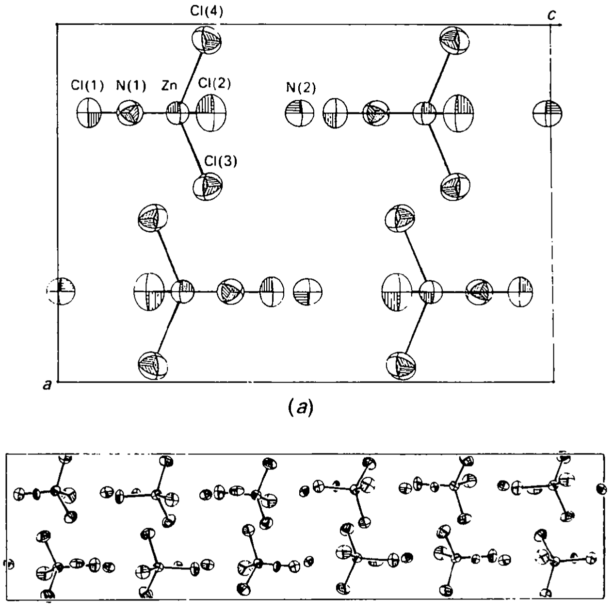

Fig. 1. (*a*) *ac* projection of the basic structure and (*b*) the threefold-modulated monoclinic phase IV of TMATC-Zn. The C atoms of the tetramethylammonium groups are omitted for clarity.

---

* See deposition footnote.

Table 3. *Distances* (Å) *and angles* (°) *of phase* IV *at* 250 K

E.s.d.'s are given in parentheses.

Zn(1)—Cl(11)	2·236 (4)	Zn(2)—Cl(21)	2·250 (4)	Zn(3)—C(31)	2·246 (3)
—Cl(12)	2·262 (4)	—Cl(22)	2·268 (4)	—Cl(32)	2·270 (3)
—Cl(13)	2·263 (3)	—Cl(23)	2·269 (3)	—Cl(33)	2·276 (3)
—Cl(14)	2·266 (3)	—Cl(24)	2·258 (3)	—Cl(34)	2·263 (3)
N(11)—C(111)	1·52 (1)	N(21)—C(211)	1·50 (2)	N(31)—C(311)	1·49 (1)
—C(112)	1·48 (1)	—C(212)	1·51 (1)	—C(312)	1·49 (1)
—C(113)	1·54 (2)	—C(213)	1·50 (2)	—C(313)	1·52 (1)
—C(114)	1·53 (1)	—C(214)	1·53 (1)	—C(314)	1·51 (1)
N(12)—C(121)	1·53 (2)	N(22)—C(221)	1·52 (1)	N(32)—C(321)	1·47 (1)
—C(122)	1·43 (2)	—C(222)	1·54 (1)	—C(322)	1·49 (2)
—C(123)	1·43 (2)	—C(223)	1·50 (2)	—C(323)	1·49 (2)
—C(124)	1·38 (2)	—C(224)	1·47 (1)	—C(324)	1·50 (2)

Cl(11)—Zn(1)—Cl(12)	111·2 (1)	C(211)—N(21)—C(212)	109·6 (9)
Cl(11)—Zn(1)—Cl(13)	109·9 (1)	C(211)—N(21)—C(213)	109·9 (9)
Cl(11)—Zn(1)—Cl(14)	109·7 (1)	C(211)—N(21)—C(214)	108·4 (9)
Cl(12)—Zn(1)—Cl(13)	107·3 (1)	C(212)—N(21)—C(213)	110·5 (8)
Cl(12)—Zn(1)—Cl(14)	110·3 (1)	C(212)—N(21)—C(214)	108·5 (8)
Cl(13)—Zn(1)—Cl(14)	109·4 (1)	C(213)—N(21)—C(214)	110·0 (9)
Cl(21)—Zn(2)—Cl(22)	110·0 (1)	C(221)—N(22)—C(222)	108·1 (7)
Cl(21)—Zn(2)—Cl(23)	109·3 (1)	C(221)—N(22)—C(223)	110·2 (8)
Cl(21)—Zn(2)—Cl(24)	108·8 (1)	C(221)—N(22)—C(224)	110·1 (8)
Cl(22)—Zn(2)—Cl(23)	108·7 (1)	C(222)—N(22)—C(223)	110·0 (8)
Cl(22)—Zn(2)—Cl(24)	109·1 (1)	C(222)—N(22)—C(224)	108·7 (8)
Cl(23)—Zn(2)—Cl(24)	109·9 (1)	C(223)—N(22)—C(224)	109·8 (8)
Cl(31)—Zn(3)—Cl(32)	111·6 (1)	C(311)—N(31)—C(312)	108·5 (8)
Cl(31)—Zn(3)—Cl(33)	109·6 (1)	C(311)—N(31)—C(313)	110·2 (8)
Cl(31)—Zn(3)—Cl(34)	108·6 (1)	C(311)—N(31)—C(314)	109·6 (8)
Cl(32)—Zn(3)—Cl(33)	108·6 (1)	C(312)—N(31)—C(313)	111·3 (8)
Cl(32)—Zn(3)—Cl(34)	108·4 (1)	C(312)—N(31)—C(314)	108·8 (8)
Cl(33)—Zn(3)—Cl(34)	110·0 (1)	C(313)—N(31)—C(314)	108·5 (8)
C(111)—N(11)—C(112)	110·7 (8)	C(321)—N(32)—C(322)	109 (1)
C(111)—N(11)—C(113)	110·6 (8)	C(321)—N(32)—C(323)	110·0 (9)
C(111)—N(11)—C(114)	107·6 (8)	C(321)—N(32)—C(324)	107·8 (8)
C(112)—N(11)—C(113)	108·7 (8)	C(322)—N(32)—C(323)	108·4 (9)
C(112)—N(11)—C(114)	109·1 (8)	C(322)—N(32)—C(324)	111·6 (9)
C(113)—N(11)—C(114)	110·1 (8)	C(323)—N(32)—C(324)	110 (1)
C(121)—N(12)—C(122)	108·9 (9)		
C(121)—N(12)—C(123)	111 (1)		
C(121)—N(12)—C(124)	110 (1)		
C(122)—N(12)—C(123)	111 (1)		
C(122)—N(12)—C(124)	108 (1)		
C(123)—N(12)—C(124)	109 (1)		

and III(lock-in). In the present case, the analysis for the atoms lying on the mirror plane in phase I can be reduced to express atom displacements in the form:

$$U_\alpha(L) = U_{0\alpha} + U_{1\alpha}\cos[(2\pi/3)(z + L) + \varphi_{1\alpha}]. \quad (1)$$

This expression describes the atomic displacements of the asymmetric unit of phase IV. Equation (1) is considered for each set of three atoms which are translationally equivalent in phase I. In (1), $L = 0$, 1, 2 stands for the three successive subcells, $\alpha = x, y, z$ refers to the three components and z represents the z component of the unique atom in the asymmetric unit of phase I to which the three atoms considered reduce when passing to phase I. Thus, the three atomic displacements are explained as the sum of a homogeneous distortion plus a sinusoidal modulation with wavevector $\mathbf{q} = (1/3)\mathbf{c}^*$. The homogeneous distortion $\mathbf{U}_0$, when considered for all the atoms in the subcell, has symmetry A_{1g} in the case of the y and z components, while the x component corresponds to a B_{3g} mode. The sinusoidal modulation along the a axis, given by the amplitudes U_{1x} and the phases φ_{1x}, describes a Σ_3 mode, whereas those corresponding to the y and z directions have the transformation properties of the irreducible representation Σ_4. This explains the large values of the atomic displacements along the a axis. The distortion mode of symmetry Σ_3 is predominant in phase IV since Σ_3 is in fact the symmetry of the order parameter which is responsible for the whole phase-transition sequence in this compound (Mashiyama, 1980).

In the case of the atoms out of the mirror plane in phase I, the decomposition (1) is incomplete for a description in terms of symmetry modes. It must be substituted by:

$$\begin{aligned} U_\alpha(L) = U_{0\alpha} &+ U_{1\alpha}\cos[(2\pi/3)(z + L) + \varphi_{1\alpha}] \\ &+ U_{2\alpha}\cos[(4\pi/3)(z + L) + \varphi_{2\alpha}] + U_{3\alpha}. \quad (2) \end{aligned}$$

The displacement $\mathbf{U}_0$ is an homogeneous distortion of A_{1g} symmetry. The other homogeneous term $\mathbf{U}_3$ represents a B_{3g} distortion, whereas the sinusoidal terms $\mathbf{U}_1$ and $\mathbf{U}_2$ correspond to distortions of symmetries Σ_3 and Σ_4 respectively. None of these modes have their corresponding atomic displacements restricted in the number of non-zero components. A complete determination of their amplitudes and phases also requires consideration of the displacements $\mathbf{U}'(1)$ of the three atoms in phase I symmetry related by the mirror plane m_x with those considered in expression (2). These displacements should satisfy for the x component:

$$\begin{aligned} U'_x(L) = -U_{0x} &+ U_{1x}\cos[(2\pi/3)(z + L) + \varphi_{1x}] \\ &- U_{2x}\cos[(4\pi/3)(z + L)\varphi_{2x}] + U_{3x} \quad (3) \end{aligned}$$

while for the y and z components:

$$\begin{aligned} U'_{y,z}(L) = U_{0y,z} &- U_{1y,z}\cos[(2\pi/3)(z + L) + \varphi_{1y,z})] \\ &+ U_{2y,z}\cos[(4\pi/3)(z + L) + \varphi_{2y,z}] - U_{3y,z}. \quad (4) \end{aligned}$$

Expressions (3) and (4) can be derived from the symmetry properties, which by definition are associated to each term in (2).

The final results along the a axis for the ions in the inorganic tetrahedra and the N atoms are given in Table 4. The Σ_3 modulation clearly constitutes the main part of the whole structural distortion. The same happens along the other two axes, where only atom Cl(3) has a Σ_3 contribution. A similar result has been observed in phase III. The Σ_3 modulation in the INC phase (II) is also given in Table 4 for comparison. It can be observed that the structure (the polarization vector) of the Σ_3 distortion in phase IV is not only essentially the same at the two temperatures investigated, but it also coincides with that of the INC phase. In other words, the phases φ_1 are maintained practically invariant, as was observed for phase III (Madariaga, Zúñiga, Pérez-Mato & Tello, 1987). Broadly speaking, the difference between the three modulations is reduced to a single common

Table 4. *Amplitudes* ($\times 10^4$) *and phases* ($\times 2\pi$) *of the harmonics describing the distortion along the a axis at* 250 K (*first line*) *and* 200 K (*second line*)

Values for the Cl(4) atom were obtained from those of Cl(3) after application of the σ_x symmetry operation. The $\Sigma_3(x)$ mode of the INC phase is also included for comparison.

	A_{1g}	Σ_3 (U_1/φ_1)	Σ_4 (U_2/φ_2)	B_{3g}	Σ_3(INC) (U_1/φ_1)
Zn		390/0·681		21	92/0·658
		474/0·681		44	
Cl(1)		443/0·836		−1	109/0·817
		563/0·842		−13	
Cl(2)		820/0·689		161	233/0·692
		968/0·683		187	
Cl(3)	−15	252/0·519	7/0·347	−5	57/0·464
	−24	334/0·542	6/0·347	−1	
N(1)		286/0·911		22	178/0·903
		376/0·903		40	
N(2)		282/0·856		−5	232/0·854
		370/0·853		−3	

Table 5. *Amplitudes and phases* ($\times 2\pi$) *of the harmonic rotations and translations describing the distortion of rigid* $ZnCl_4$ *ions at* 250 K (*first line*) *and* 200 K (*second line*)

The values for the INC phase are also included for comparison.

	R_0	R_1/φ_1	INC phase R_1/φ_1
R_x ( )	0·69	1·63/0·622	0·01/0·903
	1·35	3·30/0·623	
R_y ( )	0·64	5·53/0·523	1·97/0·512
	1·22	7·03/0·526	
R_z ( )	−2·39	11·75/0·338	7·44/0·360
	−2·70	12·92/0·340	
	T_0	T_1/φ_1	T_1/φ_1
T_x ($\times 10^4$)	36	373/0·763	180/0·774
	43	476/0·765	
T_y ($\times 10^4$)	−14	29/0·187	1/0·660
	−19	50/0·185	
T_z ($\times 10^4$)	1	10/0·510	3/0·372
	0	13/0·505	

factor which represents the amplitude of the global distortion. These results demonstrate that the predominant structural modulation corresponding to the primary-order parameter is essentially the same in phases II, III and IV. The internal structure of the modulation is maintained despite the strong symmetry changes, except for the change of wavevector and the global amplitude, which increases monotonically as the temperature decreases. The symmetry changes are due to the variation of modulation wavevector and the change of the initial phase of the modulation. This confirms from a microscopic viewpoint the assumptions made in a Landau model of these phases, where the different phases are essentially described by the amplitude and phase of a single complex parameter (order parameter) and the modulation wavevector. The relevance of secondary parameters is shown to be rather small.

Some of the data in Table 4 are implicitly correlated because of the rigidity of the inorganic $ZnCl_4$ tetrahedra. It is therefore interesting to describe the atomic displacements corresponding to these atoms in terms of small rotations and translations of these tetrahedra as rigid bodies. A fit along these lines by means of a least-squares program was successful with residues which typically amounted to 10%. The rotations obtained for the tetrahedra in three consecutive subcells can be fitted to an expression similar to (1):

$$R_\alpha(L) = R_{0\alpha} + R_{1\alpha}\cos[(2\pi/3)L + \varphi^R_{1\alpha}]. \qquad (5)$$

Something analogous can be applied to the tetrahedra translations. The results are compared in Table 5 with those obtained for the INC phase at 286 K. The homogeneous terms R_{0x}, T_{0y}, T_{0z} have A_{1g} symmetry, whereas R_{0y}, R_{0z}, T_{0x} have B_{3g} symmetry. The modulation terms R_{1y}, R_{1z}, T_{1x} correspond to Σ_3 symmetry and R_{1x}, T_{1y}, T_{1z} to Σ_4. As before, the predominance of those terms corresponding to the primary-order parameter is clear. The phases of the sinusoidal terms typically vary less than a degree from 250 to 200 K, and in the case of the Σ_3 terms they essentially coincide with those observed in the INC phase. The phases corresponding to the Σ_4 terms have, however, no clear correlation with those observed in the INC phase. The amplitudes of these terms in the INC phase are practically two orders of magnitude smaller than those of the Σ_3 distortion. Hence the present result seems to indicate that these values have little physical significance and were probably an artefact of the refinement process.

References

Cosier, J. & Glazer, A. M. (1986). *J. Appl. Cryst.* **19**, 105–107.

Cromer, D. T. & Liberman, D. (1970). *J. Chem. Phys.* **3**, 1891–1898.

Cromer, D. T. & Mann, J. B. (1968). *Acta Cryst.* **A24**, 321–324.

Hogervorst, A. C. R. & Helmholdt, R. B. (1988). *Acta Cryst.* **B44**, 120–128.

Madariaga, G., Zúñiga, F. J., Pérez-Mato, J. M. & Tello, M. J. (1987). *Acta Cryst.* **B43**, 356–368.

Mashiyama, H. (1980). *J. Phys. Soc. Jpn*, **40**, 2270–2277.

Pérez-Mato, J. M., Gaztelua, F., Madariaga, G. & Tello, M. J. (1986). *J. Phys. C*, **19**, 1923–1935.

Ruiz-Larrea, I., Lopez-Echarri, A. & Tello, M. J. (1981). *J. Phys. C*, **14**, 3171–3176.

Stewart, J. M., Kruger, G. J., Ammon, H. L., Dickinson, C. & Hall, S. R. (1972). The *XRAY* system – version of June 1972. Tech. Rep. TR-192. Computer Science Center, Univ. of Maryland, College Park, Maryland, USA.

Tanisaki, S. & Mashiyama, H. (1980). *J. Phys. Soc. Jpn*, **48**, 339–340.

Wiesner, J. R., Srivastava, R. C., Kennard, C. H. L., Di Vaira, M. & Lingafelter, E. C. (1967). *Acta Cryst.* **23**, 565–574.